HHS Public Access

Author manuscript

Nanoscale. Author manuscript; available in PMC 2016 July 28.

Published in final edited form as:

Nanoscale. 2015 July 28; 7(28): 12038–12044. doi:10.1039/c5nr01407g.

Bio-Inspired Synthesis of Hybrid Silica Nanoparticles Templated from Elastin-like Polypeptide Micelles

Wei Han[1,3], **Sarah MacEwan**[1,3], **Ashutosh Chilkoti**[1,2,3], and **Gabriel P. López**[1,2,3,*]

[1]Department of Biomedical Engineering, Duke University, Durham, North Carolina 27708

[2]Department of Mechanical Engineering and Materials Science, Duke University, Durham, North Carolina 27708

[3]Research Triangle Materials Science and Engineering Center, Durham, North Carolina, 27708

Abstract

The programmed self-assembly of block copolymers into higher order nanoscale structures offers many attractive attributes for the development of new nanomaterials for numerous applications including drug delivery and biosensing. The incorporation of biomimetic silaffin peptides in these block copolymers enables the formation of hybrid organic-inorganic materials, which can potentially enhance the utility and stability of self-assembled nanostructures. We demonstrate the design, synthesis and characterization of amphiphilic elastin-like polypeptide (ELP) diblock copolymers that undergo temperature-triggered self-assembly into well-defined spherical micelles. Genetically encoded incorporation of the silaffin R5 peptide at the hydrophilic terminus of the diblock ELP leads to presentation of the silaffin R5 peptide on the coronae of the micelles, which results in localized condensation of silica and the formation of near-monodisperse, discrete, sub-100 nm diameter hybrid ELP-silica particles. This synthesis method, can be carried out under mild reaction conditions suitable for bioactive materials, and will serve as the basis for the development and application of functional nanomaterials. Beyond silicification, the general strategies described herein may also be adapted for the synthesis of other biohybrid nanomaterials as well.

Introduction

Several biologically inspired methodologies for the facile synthesis of silica have been developed,[1–4] and the discovery of peptides,[5–7] proteins,[8, 9] and polymers[10–12] that facilitate the polymerization of silica under physiologically relevant conditions at controllable rates has expanded the utility of silica-stabilized organic materials. Two of the most prevalent biomimetic silica precipitants are polyamines and polypeptides that contain numerous lysine residues (e.g. poly-L-lysine), which have been used to template the formation of siliceous materials with various morphologies.[12–16] Kröger *et al* first reported the identification and characterization of silaffins —peptides with *silica affinity*— which are a group of polycationic peptides based on motifs isolated from the diatom *Cylindrotheca fusiformis* that enable the diatom to form its silica cell walls.[5] Study of gene sequences revealed a sequence

*Correspondence: gabriel.lopez@duke.edu.

of 265 amino acids containing seven homologous peptides that catalyzed biosilicification. These peptides, containing a high number of cationic residues (lysine and arginine), precipitate silica particles (of approximately 500 to 700 nm in diameter) under physiological conditions in a manner that depends on the concentration of the protein and solution pH. The same group also reported post-translational phosphorylation of the serine residues in the silaffin and modification of lysine residues with long-chain polyamines, and hypothesized that these post-translational modifications play an important role in silaffin-mediated silica condensation reactions.[6] However, the silaffin R5 peptide (see below for sequence) that is not post-translationally modified facilitates silicification in phosphate buffer.[6, 17] Its lack of post-translational modification makes it an appealing candidate for applications in which it can be encoded in commonly used expression systems such as *E. coli*. The reported mechanism for silica mineralization of the silaffin R5 peptide depends on crosslinking of silaffin chains through solvent phosphate groups and presentation of a high density of cationic charges to favor silica condensation around the peptide.[17] The applications of this peptide have resulted in numerous demonstrations of silicification.[18–22] However, the uncontrolled self-assembly of these R5 polypeptide templates prior to silica deposition often results in a network of fused silica nanoparticles.

Herein, we demonstrate that silaffin R5 peptides fused to elastin-like polypeptides (ELPs) that self-assemble into monodisperse micelles can be used as templates for the controlled deposition of near-monodisperse silica nanoparticles. ELPs are a family of peptide polymers composed of the repeating pentapeptide sequence VPGXG, where X is the guest residue, which can be any amino acid except Pro (P). ELPs exhibit an aqueous lower-critical solution temperature (LCST) transition that is dependent on intrinsic material parameters, such as the ELP's guest residue (X),[23, 24] molecular weight, and concentration,[25] and extrinsic environmental factors, such as the type and concentration of salt.[23, 26, 27] ELPs can be encoded at the genetic level, expressed at high yield in *E. coli* and purified by exploiting their LCST behavior to produce monodisperse polypeptides that are entirely of the same composition, length, and physical properties. In addition, the ability to precisely encode complex block architectures at the gene level affords the possibility of creating polypeptides of enormous complexity with tight control. Chilkoti *et al*. have demonstrated in several previous papers that ELP block copolymers comprised of different ELP sequences with distinct LCSTs can form micellar structures within specific temperature ranges and can be used for applications such as drug delivery[28–30] and biosensing.[26, 31–33] Diblock ELP sequences have been previously designed to incorporate moieties appended to the hydrophilic ELP block, resulting in functionally decorated micelles, without disruption to the self-assembly process.[28, 32, 34] In addition, conjugation of amino acids in ELPs with hydrophobic small molecules and drugs has also led to self-assembly into nanoparticles.[35, 36]

Here we show a proof of concept that, by appending the silaffin R5 peptide to the hydrophilic terminus of an ELP diblock copolymer, the resulting polypeptide maintains its ability to self-assemble into micelles and is able to serve as an effective template for silicification and the formation of near-monodisperse silica nanoparticles. ELPs are an attractive fusion partner for silica promoting polypeptides because they can be easily

programmed at the genetic level to contain R5 or other polypeptides, produce assembled templates that are highly uniform in composition and size, and can be easily expressed and purified easily and rapidly, resulting in large quantities of these hybrid materials. In addition, the modular design of ELPs can allow for additional control of silica morphologies based on its ELP template assemblies. Further, the encapsulation and retention of designed ELPs within the silica-polypeptide hybrids allow for facile loading of other molecular entities as well as control of particle size. These results set the stage for the synthesis of uniform hybrid ELP and silica nanoparticles for future applications such as drug delivery.

Materials and Methods

Materials

Restriction enzymes BglI, NdeI, BseRI, AcuI, BamHI and XbaI, T4 DNA Ligase and calf intestinal phosphatase (CIP) were purchased from New England Biolabs (Ipswich, MA). pET-24a(+) vector was purchased from Novagen Inc. (Madison, WI). BL21 *E. coli* competent cells were purchased from EdgeBio (Gaithersburg, MD). Oligonucleotides were obtained from Integrated DNA Technologies, Inc. (Coralville, IA). Terrific Broth was purchased from MO BIO Labs, Inc. (Carlsbad, CA) and SDS-PAGE gels from BioRad, Inc. (Hercules, CA). Tetramethylorthosilicate (TMOS) was used as the silica precursor for condensation reactions and was obtained from Alfa Aesar (Ward Hill, MA). Quantifoil 300 mesh copper support grids (657-300-Cu) for cryogenic transmission electron microscopy were purchased from Electron Microscopy Sciences (Hatfield, PA). Alexa Fluor 488 Fluorescent Dye was purchased from Life Technologies (Carlsbad, CA).

Assembly of ELP-R5 silaffin gene

The ELP and silaffin R5-ELP (herein referred to as ELP-R5) genes were assembled by recursive directional ligation by plasmid reconstruction (PRe-RDL).[37] The diblock gene encodes for 60 pentapeptide repeats with the guest residue valine as the hydrophobic (core) block and 60 pentapeptide repeats with the guest residues alanine and glycine in a 1:1 ratio as the hydrophilic (corona) block. A leader DNA sequence that encodes for MGCGWP was incorporated, so as to include a unique cysteine (C) for thiol-mediated conjugation of Alexa Fluor 488 and a tryptophan (W) for quantification of the ELP by UV-vis spectrophotometry at 280 nm. A pET-24a(+) vector encoding the ELP sequence was isolated from *E. coli* cells and purified by miniprep. Another pET-24a(+) vector containing the silaffin R5 sequence was obtained by insertion of designed oligonucleotides, encoding R5 silaffin, into an empty vector, as previously described.[23] PRe-RDL was performed by digestion of the ELP-encoding vector with AcuI and BglI restriction enzymes, digestion of silaffin-R5-encoding vector with BseRI and BglI, and gel isolation of the desired DNA fragments from each restriction digestion. T4 DNA ligase was used to ligate vector segments encoding the ELP sequence and silaffin R5 and the ligated plasmid was transformed into BL21(DE3) *E. coli* for expression. The gene for a control ELP (ELP-GG), without the trailing silaffin sequence, was similarly constructed.

Expression and purification of ELP-R5 silaffin

Expression of ELP-R5 and ELP-GG was carried out in *E. coli* containing the assembled plasmids as described previously.[37] Fresh Terrific Broth (TB) culture media was prepared at 55 g/L, autoclaved and supplemented with 45 mg/mL kanamycin. A hyperexpression protocol was used for ELP expression that relies on the inherent leakiness of the T7 promoter.[31] A single colony of *E. coli* harboring an expression plasmid that encodes for an ELP of interest was used to inoculate a 50 mL starter culture in TB. After one day of culture at 37 °C at 200 rpm, cells were centrifuged the following day and resuspended in 10 mL of fresh TB and transferred into 1 liter TB and cultured at 37 °C and 200 RPM rotation for 24 h. Cells were then centrifuged, resuspended in phosphate buffered saline (PBS; pH 7.4) and lysed by sonication. Purification of ELP-R5 was carried out by inverse transition cycling (ITC), as previously described.[38] Briefly, one cycle of ITC consists of addition of NaCl and increase of temperature until solution becomes turbid, indicating that the ELP has transitioned, followed by centrifugation at 25 °C and 15,000 × g for 10 minutes to pellet the ELP, and resuspension of the pellet in fresh PBS or water. This step is followed by centrifugation at 4 °C and 15,000 × g for 10 minutes to remove irreversibly aggregated material, the supernatant is transferred to a new tube. Three cycles of ITC were sufficient to produce pure ELP-R5 polypeptides, as characterized by SDS-PAGE.

Silica deposition using the method of Kröger et al

Silica deposition was carried out using methods similar to those previously described by Kröger *et al*.[6] For all reactions, 2.5 mg/mL final concentration of ELP-R5 (or ELP-GG control) in PBS or water was prepared and incubated at 37 °C for 15 min prior to reaction to ensure micelle formation. 1 M TMOS hydrolyzed in 1 mM HCl was prepared and mixed for 10 min by rotation at room temperature. The ELP-R5 solution was diluted to the final concentration and then hydrolyzed TMOS was added to the appropriate final TMOS concentration. The mixture was allowed to react for a set period of time, before centrifugation at 10,000 × g and resuspended in DI water.

Conjugation of fluorescent dye to ELP

Fluorescently conjugated ELP was prepared by reaction of the single cysteine residue in ELP-R5 (or ELP-GG), with Alexa Fluor 488-maleimide. 100 μM ELP-R5 (or ELP-GG) was prepared in PBS at room temperature and then a ten-fold excess of tris(2-carboxyethyl)phosphine (TCEP) was added to reduce disulfide bonds. A 10 mM stock solution of Alexa Fluor 488-maleimide was prepared and reacted with ELP-R5 (or ELP-GG control) at a molar ratio of fluor:ELP of 10:1. The reaction was allowed to continue for 12 h at 4 °C, the reaction mixture was then dialyzed using a 10K MWCO dialysis membrane (Thermo Scientific) to remove unreacted dye.

Characterization of silica encapsulation of ELP-R5

UV-vis spectrophotometry was performed on a Cary 300 UV-vis spectrophotometer (Agilent, Santa Clara, CA). 500 μL of a 20 μM ELP-R5 solution in water was aliquoted into a quartz crystal cuvette and placed into the sample well. The temperature dependent absorbance of the sample at 350 nm was measured from 20 °C to 60 °C at 0.1 °C increments

and at a rate of 1 °C/min. Dynamic light scattering (DLS) was carried out on a DynaPro Plate Reader II (Wyatt Technology, Santa Barbara, CA). Measurements of hydrodynamic radii were made in triplicate, with each datum consisting of 10 acquisitions for 5 s each. The autocorrelation function was fitted by a regularization algorithm provided by the manufacturer to determine the hydrodynamic radius (R_h) of the ELPs. Zeta potential was measured on a Zetasizer Nano ZS (Malvern, UK) with 90° scattering optics. 900 μL of an ELP solution was placed into a mini-quartz cuvet, and measured three times for each condition. Three measurements were then averaged to create a single datum. Cryo-transmission electron microscopy (cryo-TEM) was performed on a Tecnai G^2 Twin (FEI, Hillsboro, OR) at 200 keV. Samples were vitrified for cryo-TEM on a Vitrobot Mark III (FEI) using a 3 s blot time at −3 blot offset for all samples and imaged at a maximum of 15 electrons/$Å^2$ per image. Fluorescence microscopy was performed a Zeiss Axio Observer with temperature and humidity control with a 100×/1.45 oil Plan Apochromat DIC objective.

Results and Discussion

Figure 1A and B present a schematic and the amino acid sequence of the diblock ELP-R5 silaffin peptide. Raising the temperature above the critical micellization temperature (CMT) of ELP-R5 triggers its self-assembly into spherical micelles (Figure 1C), leading to the presentation of multiple copies of the R5 peptide on the corona of the micelle. We hypothesized that the presentation of a high local density of positively-charged residues in the silaffin R5 peptide at the corona of the micelle would selectively trigger the mineralization of silica (Figure 1C).

We first characterized ELP-R5 to examine its self-assembly into spherical micelles and compared it to a diblock ELP-GG (negative control without silaffin) to determine whether appending the silaffin R5 peptide on the terminus of the ELP affects self-assembly. SDS-PAGE of purified ELP-R5 (Figure 2a Lane 2) was consistent with its theoretical molecular weight (49.8 kDa), as was the case for the ELP-GG construct (Figure 2a Lane 3; 47.8 kDa). To determine the effect of the silaffin R5 peptide on micellization, we performed temperature-dependent turbidimetry and dynamic light scattering (DLS) measurements on a 25 μM solution of ELP-R5 in water (Figure 2b). The data show a slight increase in turbidity at approximately 33 °C, which is indicative of micelle formation,[31] followed by a large increase in absorbance between 55 °C and 60 °C, resulting from the hydrophobic collapse of the coronal block and subsequent bulk aggregation of the ELP-R5 into micron size aggregates.[31] The temperature-dependent turbidity is in agreement with DLS measurements that show a similar increase in hydrodynamic radius (R_h) from ~9 nm (unimer) to 25 nm (micelle) at approximately 33 °C. In addition, the formation of micelles from ELP-R5 was reversible, such that micelles disassemble upon lowering the solution temperature below the T_t (data not shown), consistent with previous results obtained for similar systems.[35] These data are consistent with those measured for the control ELP-GG that does not contain the silaffin R5 peptide (Figure S1A and S1B) and indicate a small to negligible effect on micelle formation from attachment of the silaffin R5 peptide to the ELP (Figure S1C). These results suggest that micelle formation presents the silaffin R5 peptide on the corona of the micelle

at a relatively high local concentration that we hypothesized should facilitate the condensation of silica.

To test this hypothesis, we next carried out silicification experiments to examine the formation of silica nanoparticles. Silicification reactions were first carried out in phosphate buffer using the method of Kröger *et al.* (see Methods) at 37 °C for 30 s. These conditions resulted in the formation of clusters of relatively large fused spheres of silica with dimensions between 300 and 800 nm in diameter for ELP-R5 constructs (Figure S2). By contrast control experiments with the ELP-GG resulted in unappreciable formation of silica particles. This result is in agreement with previous studies that concluded that the assembly of silaffin mediated by the RRIL terminating sequence[17] in phosphate-containing solutions results in the formation and deposition of silica upon addition of silicic acid to form large, highly polydisperse and fused silica particles. Indeed, we suggest a similar mechanism in this circumstance, i.e., that silaffin R5-conjugated ELP is crosslinked through electrostatic interactions in the presence of phosphate anions and that the addition of silicic acid to this solution of assembled templates results in silica polycondensation.[6, 17] To demonstrate that ELP-R5 is encapsulated within the silica particles as a result of the silicification reaction, we conjugated fluorescent Alexa Fluor 488 to the single cysteine of ELP-R5, and carried out the same silicification reactions. We then analyzed the resulting samples by fluorescence microscopy (Figure S3). Comparison of the differential interference contrast (DIC) images with the fluorescence images shows that the resulting silica particles align with the fluorescent signal emitted by the Alexa Fluor 488, suggesting the presence of fluorescent ELP-R5 within the fused silica particles. This result provides evidence that it is possible to employ ELP fusions with silaffin R5 to template the formation and arrangement of silica deposition and that their formation in phosphate buffer was driven by the mechanism described above.

We next hypothesized that a predetermined, controlled assembly of highly-monodisperse, micellar templates for silica deposition using ELP constructs, presenting silaffin peptides at the coronae accomplished without the addition of phosphate in solution, would lead to silica nanoparticles that are similarly individualized and monodisperse. We incubated solutions of ELP-R5 micelles in water with TMOS for varying periods of time at 37°C (a temperature that is greater than the CMT of ELP-R5 in water) and characterized the reaction products by cryo-TEM and light scattering. Cryo-TEM showed that the silica particles obtained by reaction 100 mM TMOS in the presence of ELP-R5 (2.5 mg/mL) at 37°C for 8 h are of uniform size and discrete (i.e., not fused together as observed for reactions in the presence of phosphate ion, Figure 3A and 3B). Interestingly, the uniform particles are packed in a roughly hexagonal lattice within the vitreous ice; the lack of particles near the center of the grid hole is likely due to a decrease in the thickness of vitreous ice within the grid hole. Image analysis of >200 particles throughout the grid showed that the silica nanoparticles are near monodisperse in size with a mean diameter of 51 ± 4.8 nm. Analysis of contrast along the radial axis of individual particles suggests significant silica penetration into the ELP micelles. The resulting silica nanoparticles do not exhibit a core-shell structure as previously observed with templated silica particles[12], and appear to be solid and similar to those studied by Thomassen *et al.*, which were prepared by ammonia or lysine catalyzed hydrolysis and

polycondensation reactions.[39] Furthermore, zeta potential measurements for ELP-GG control micelles and ELP-R5 micelles in solution at pH 7 prior to, and post silicification were obtained (Figure 3C). In contrast to ELP-R5 micelles alone (middle), which exhibit a positive zeta potential of 8.1 ± 0.7 mV, hybrid ELP-R5 silica particles formed through exposure to 100 mM TMOS for 8 hours resulted in a zeta potential of −27.1 ± 3.0 mV, due to the deposition of silica around the micelles and associated negative surface charge of deprotonated silanol groups. DLS measurements were also taken in a time-course study of the formation of silica on ELP-R5 (Figure 4A) using three different final TMOS concentrations – 10 mM, 50 mM and 100 mM – with the concentration of ELP-R5 held constant for each reaction. The R_h increased from ~25 nm before the reaction to ~35 nm for each of the three concentrations. The discrepancy between the measured hydrodynamic size through DLS and the observed size through cryo-TEM of the ELP/silica particles may be due to the fact that R_h is calculated from correlation to particles with an equivalent diffusion coefficient, which may be overestimated for denser, inorganic particles compared to polymer materials, and that R_h accounts for the solvation layer dimension while electron microscopy solely visualizes the particle size in solution.[40, 41] Interestingly, at all TMOS concentrations studied, there is a general trend in the data that suggests that the growth in the size of the nanoparticles upon silicification occurs during the first hour of measurement, after which no further significant increase in measured R_h is observed. With regards to excess silica precursor within each reaction, we hypothesize that the formation of silica particles under the conditions of this study is dependent on the availability of a high density of cationic charges from ELP-R5 micelles. Away from these reaction centers, it is likely that the rate of condensation relative to hydrolysis is insufficient to promote the formation of silica and thus does not result in observable silica material within the experimental timescale.

Importantly, we found the uniform silicification and formation of hybrid nanoparticles to be dependent on both the presence of the silaffin R5 peptide and the micelles (Figure 4B). While the ELP-R5 micelles resulted in a formation of hybrid particles of uniform size, both the ELP-GG control micelle without silaffin R5 peptide and the unassembled ELP-R5 unimer (i.e. silicified at 25°C, a temperature that is below the CMT of 33 °C of ELP-R5 in water) resulted in a lack of silica particles under nearly identical experimental conditions. This is strong evidence that the presentation of a high local density of positive charges from the lysine and arginine residues of the silaffin R5 through micellization of the ELP-R5 construct is necessary to serve as growth centers for silica deposition on the nanoparticles.

Conclusion

We report the synthesis of discrete and monodisperse nanoparticles containing silica and an engineered polypeptide in a temperature- and assembly- dependent manner. By combining the temperature-triggered self-assembly of ELPs into monodisperse micelles with the silicification properties of the silaffin R5 peptide in water, we demonstrate the formation of very uniform, hybrid silica-polypeptide nanoparticles using a simple, isothermal reaction that may be suitable for biomedical or biotechnological applications. For example, this method is promising for encapsulation of therapeutic or imaging moieties within silica stabilized ELP nanoparticles. Furthermore, conjugation of the silaffin R5 to other self-

assembling peptides that provide access to diverse nanoparticle morphologies may enable the facile synthesis of silica stabilized hybrid particles of various sizes and morphologies. Finally, the design of more complex, functional, self-assembling ELPs that incorporate spatially-specific or multiple biomineralization-promoting tags may enable the fabrication of more complex hybrid nanomaterials.

Supplementary Material

Refer to Web version on PubMed Central for supplementary material.

Acknowledgements

This work is supported by NSF's Research Triangle MRSEC (DMR-1121107). W.H. acknowledges support through a NIH Biotechnology Predoctoral Training Fellowship and the Center for Biological and Tissue Engineering (NIH Grant No. 5T32GM008555-18). The authors thank the staff of the Duke University Shared Materials Instrumentation Facility and Light Microscopy Core Facility for their expert technical assistance.

References

1. Patwardhan SV. Chemical Communications. 2011; 47:7567–7582. [PubMed: 21479320]
2. Patwardhan SV, Clarson SJ, Perry CC. Chemical Communications. 2005:1113–1121. [PubMed: 15726164]
3. Betancor L, Luckarift HR. Trends in Biotechnology. 2008; 26:566–572. [PubMed: 18757108]
4. Dickerson MB, Sandhage KH, Naik RR. Chemical Reviews. 2008; 108:4935–4978. [PubMed: 18973389]
5. Kröger N, Deutzmann R, Sumper M. Science. 1999; 286:1129–1132. [PubMed: 10550045]
6. Kroger N, Lorenz S, Brunner E, Sumper M. Science. 2002; 298:584–586. [PubMed: 12386330]
7. Wenzl S, Hett R, Richthammer P, Sumper M. Angewandte Chemie. 2008; 120:1753–1756.
8. Shimizu K, Cha J, Stucky GD, Morse DE. Proceedings of the National Academy of Sciences. 1998; 95:6234–6238.
9. Cha JN, Shimizu K, Zhou Y, Christiansen SC, Chmelka BF, Stucky GD, Morse DE. Proceedings of the National Academy of Sciences. 1999; 96:361–365.
10. Kröger N, Deutzmann R, Bergsdorf C, Sumper M. Proceedings of the National Academy of Sciences. 2000; 97:14133–14138.
11. Yuan JJ, Jin RH. Advanced materials. 2005; 17:885–888.
12. Yuan J-J, Mykhaylyk OO, Ryan AJ, Armes SP. Journal of the American Chemical Society. 2007; 129:1717–1723. [PubMed: 17249673]
13. Jan J-S, Lee S, Carr CS, Shantz DF. Chemistry of Materials. 2005; 17:4310–4317.
14. Jan J-S, Shantz DF. Advanced materials. 2007; 19:2951–2956.
15. Bernecker A, Wieneke R, Riedel R, Seibt M, Geyer A, Steinem C. Journal of the American Chemical Society. 2009; 132:1023–1031. [PubMed: 20041715]
16. Li Y, Du J, Armes SP. Macromolecular rapid communications. 2009; 30:464–468. [PubMed: 21706626]
17. Knecht MR, Wright DW. Chemical Communications. 2003:3038. [PubMed: 14703846]
18. Brott LL, Naik RR, Pikas DJ, Kirkpatrick SM, Tomlin DW, Whitlock PW, Clarson SJ, Stone MO. Nature. 2001; 413:291–293. [PubMed: 11565027]
19. Luckarift HR, Spain JC, Naik RR, Stone MO. Nat Biotech. 2004; 22:211–213.
20. Naik RR, Tomczak MM, Luckarift HR, Spain JC, Stone MO. Chemical Communications. 2004:1684–1685. [PubMed: 15278136]
21. Marner WD, Shaikh AS, Muller SJ, Keasling JD. Biotechnology Progress. 2009; 25:417–423. [PubMed: 19334285]

22. Wong Po Foo C, Patwardhan SV, Belton DJ, Kitchel B, Anastasiades D, Huang J, Naik RR, Perry CC, Kaplan DL. Proceedings of the National Academy of Sciences of the United States of America. 2006; 103:9428–9433. [PubMed: 16769898]
23. McDaniel JR, Radford DC, Chilkoti A. Biomacromolecules. 2013; 14:2866–2872. [PubMed: 23808597]
24. Urry DW, Luan CH, Parker TM, Gowda DC, Prasad KU, Reid MC, Safavy A. Journal of the American Chemical Society. 1991; 113:4346–4348.
25. Meyer DE, Chilkoti A. Biomacromolecules. 2004; 5:846–851. [PubMed: 15132671]
26. MacEwan SR, Chilkoti A. Biopolymers. 2010; 94:60–77. [PubMed: 20091871]
27. Cho Y, Zhang Y, Christensen T, Sagle LB, Chilkoti A, Cremer PS. The Journal of Physical Chemistry B. 2008; 112:13765–13771. [PubMed: 18842018]
28. MacEwan SR, Chilkoti A. Nano Letters. 2014; 14:2058–2064. [PubMed: 24611762]
29. Shi P, Aluri S, Lin Y-A, Shah M, Edman M, Dhandhukia J, Cui H, MacKay JA. Journal of Controlled Release. 2013; 171:330–338. [PubMed: 23714121]
30. Shah M, Edman MC, Janga SR, Shi P, Dhandhukia J, Liu S, Louie SG, Rodgers K, MacKay JA, Hamm-Alvarez SF. Journal of Controlled Release. 2013; 171:269–279. [PubMed: 23892265]
31. Dreher MR, Simnick AJ, Fischer K, Smith RJ, Patel A, Schmidt M, Chilkoti A. Journal of the American Chemical Society. 2007; 130:687–694. [PubMed: 18085778]
32. MacEwan SR, Chilkoti A. Nano Letters. 2012; 12:3322–3328. [PubMed: 22625178]
33. Ghoorchian A, Chilkoti A, López GP. Analytical Chemistry. 2014; 86:6103–6110. [PubMed: 24832919]
34. Hassouneh W, Fischer K, MacEwan SR, Branscheid R, Fu CL, Liu R, Schmidt M, Chilkoti A. Biomacromolecules. 2012; 13:1598–1605. [PubMed: 22515311]
35. McDaniel JR, Bhattacharyya J, Vargo KB, Hassouneh W, Hammer DA, Chilkoti A. Angewandte Chemie. 2013; 52:1683–1687. [PubMed: 23280697]
36. MacKay JA, Chen M, McDaniel JR, Liu W, Simnick AJ, Chilkoti A. Nature materials. 2009; 8:993–999.
37. McDaniel JR, MacKay JA, Quiroz FGa, Chilkoti A. Biomacromolecules. 2010; 11:944–952. [PubMed: 20184309]
38. Hassouneh W, Christensen T, Chilkoti A. Current Protocols in Protein Science. 2001; 61:6.11.11–16.11.16.
39. Thomassen LCJ, Aerts A, Rabolli V, Lison D, Gonzalez L, Kirsch-Volders M, Napierska D, Hoet PH, Kirschhock CEA, Martens JA. Langmuir. 2009; 26:328–335. [PubMed: 19697952]
40. Olariu CI, Yiu HH, Bouffier L, Nedjadi T, Costello E, Williams SR, Halloran CM, Rosseinsky MJ. Journal of Materials Chemistry. 2011; 21:12650–12659.
41. De Palma R, Peeters S, Van Bael MJ, Van den Rul H, Bonroy K, Laureyn W, Mullens J, Borghs G, Maes G. Chemistry of Materials. 2007; 19:1821–1831.

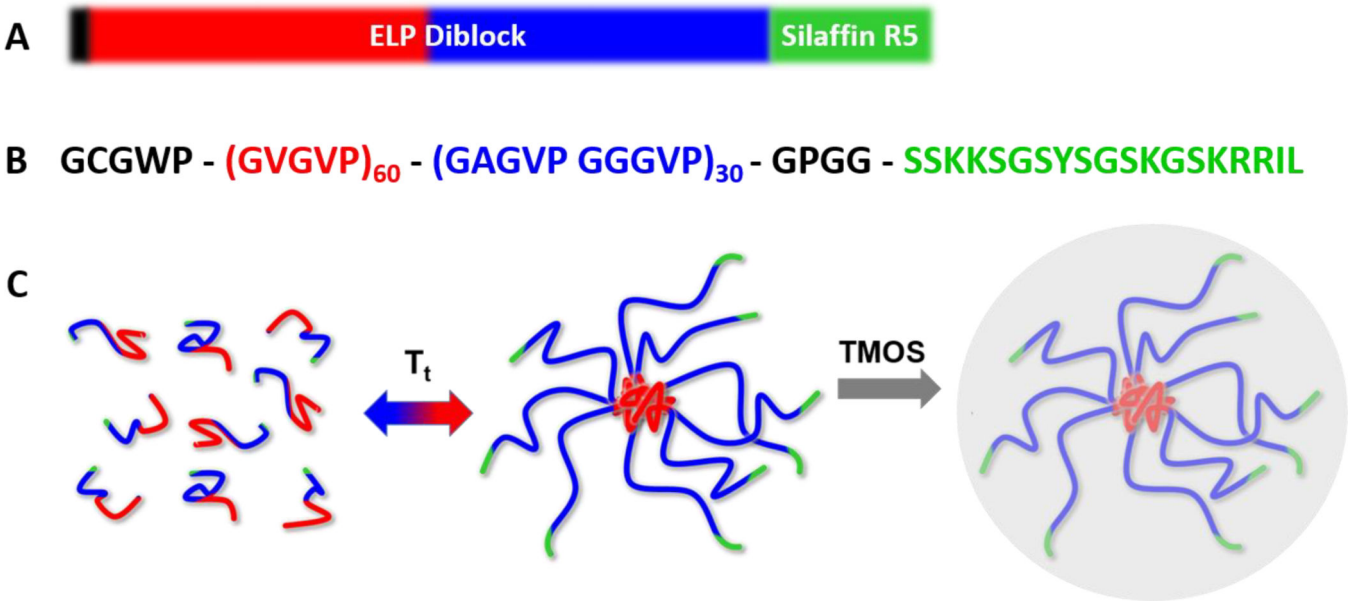

Figure 1.

Schematic representation of materials and method. (A) Representation of ELP-R5 diblock polymer with a C-terminal silaffin R5 peptide; the hydrophobic ELP block is in red and the hydrophilic ELP block is in blue. (B) Amino acid sequence for ELP-R5 containing leader, sequence at the N-terminus for conjugation of fluorophore (black), hydrophobic ELP block (red), hydrophilic ELP block (blue), and silaffin R5 peptide (green). (C) Representation of the reaction process proceeding from assembly of ELP constructs into micelles in solution, followed by addition of TMOS to produce silica nanoparticles.

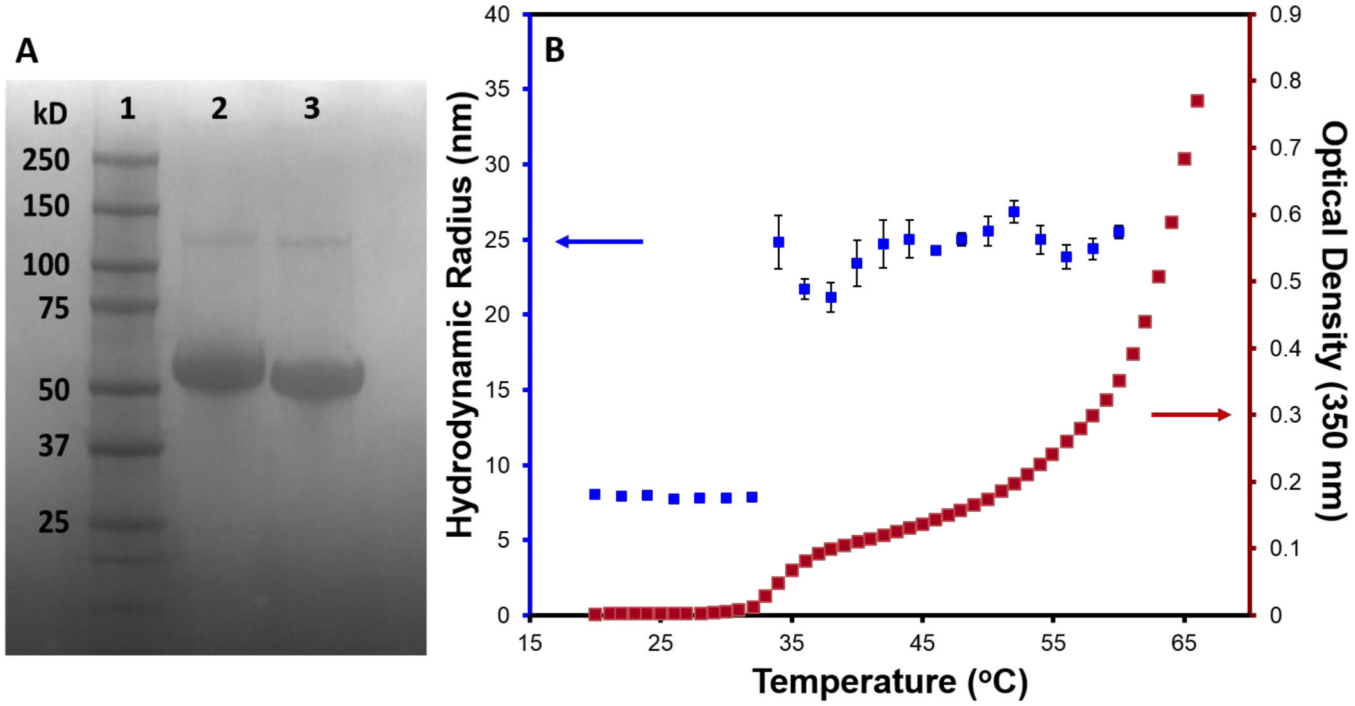

Figure 2.

Characterization of ELP-R5. (A) SDS-PAGE gel with molecular weight ladder (lane 1), ELP-R5 (lane 2), and control ELP-GG (lane 3). (B) Dynamic light scattering (DLS) and turbidity measurement for 25 μM ELP-R5 in water as a function of solution temperature. The R_h measured by DLS is plotted on the left vertical axis (blue) and the optical density at 350 nm (turbidity) is plotted on the right vertical axis (red).

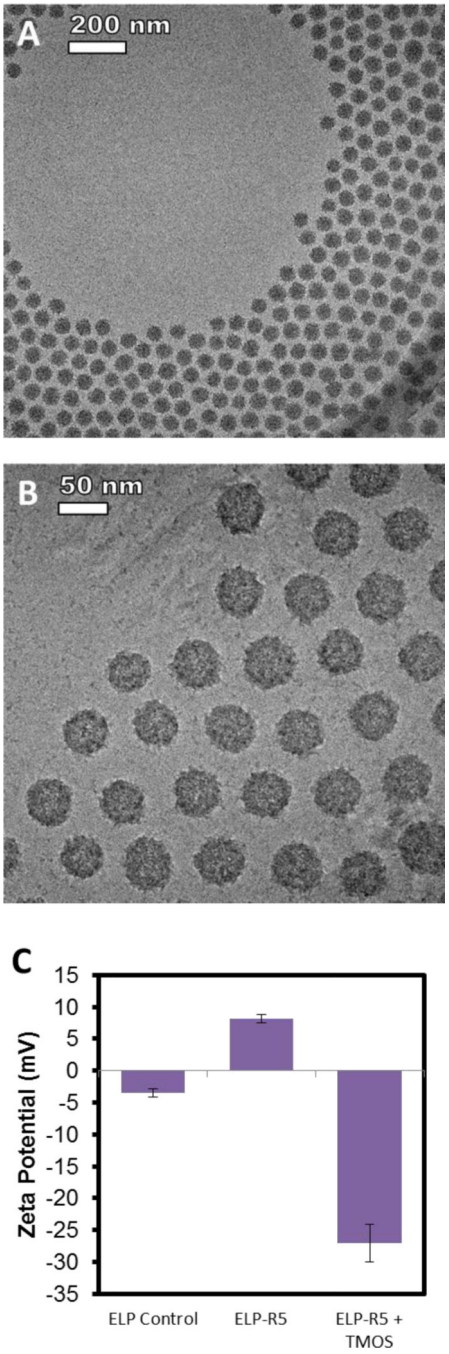

Figure 3.

Characterization of silicification of ELP-R5 micelles. (A, B) Cryo-TEM images of ELP-R5 micelle templated silica nanoparticles by reaction with 100 mM hydrolyzed TMOS at 37 °C for 8 h. Scale bars are 200 nm (A) and 50 nm (B). (C) Zeta potential measurement of nanoparticles at pH 7 of control ELP-GG micelles (left), ELP-R5 micelles without exposure to TMOS (center) and particles formed by exposure of ELP-R5 micelles to TMOS (right, same reaction conditions as A, B).

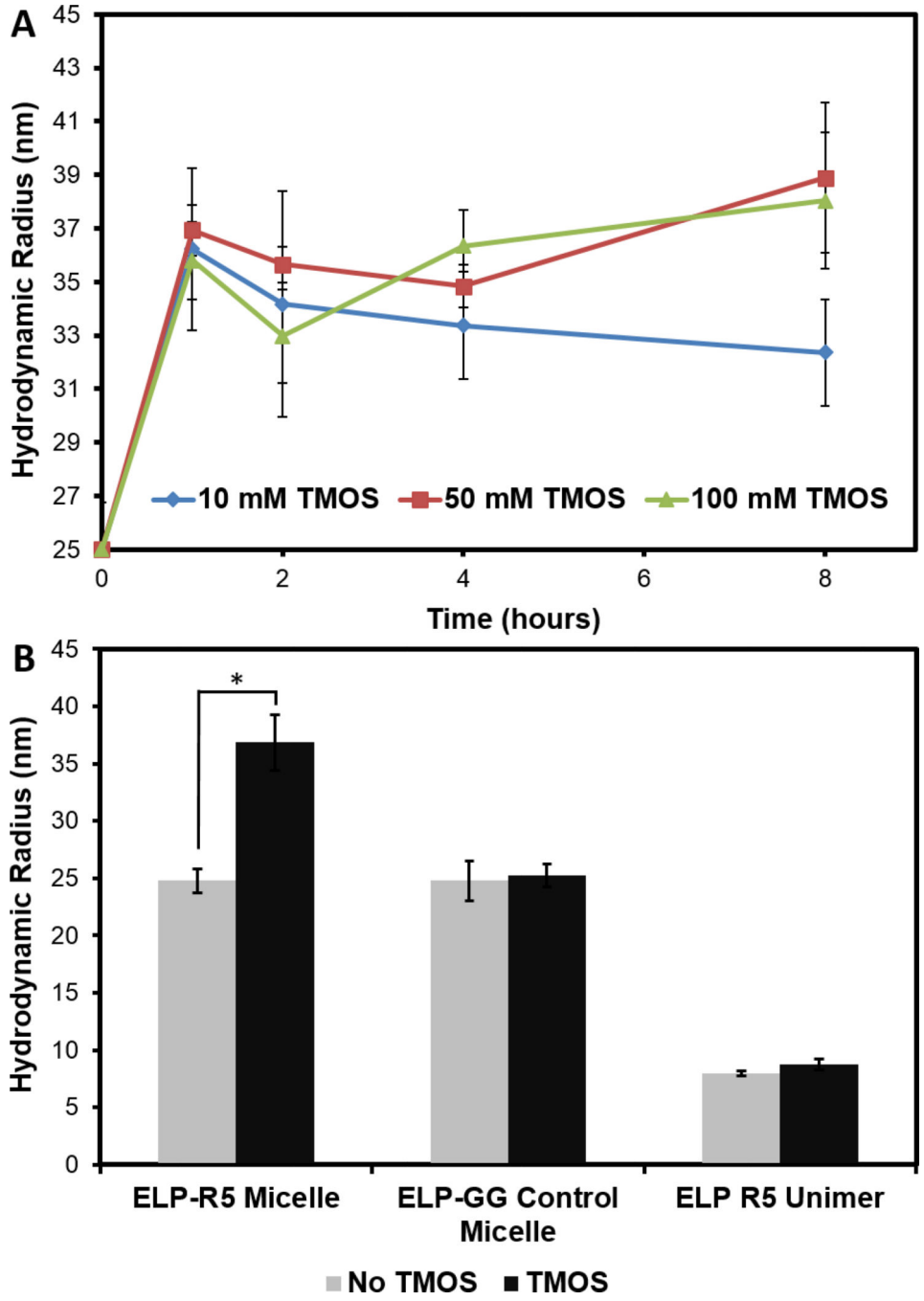

Figure 4.

(A) Time course measurements of hydrodynamic radii of ELP-R5 with 10 mM (circles, blue), 50 mM (squares, red) and 100 mM (triangles, green) TMOS. (B) Hydrodynamic radii of ELPs prior to (left, orange bars) and after (right, purple bars) incubation with 100 mM hydrolyzed TMOS for 8 h. *ELP-R5 micelles prior to and after silicification showed a significant difference in size ($p < 0.05$, Student's t-test).